

Δ -Excitation and Exchange Corrections for NN-Bremsstrahlung

M. Jetter and H. W. Fearing
*TRIUMF, 4004 Wesbrook Mall, Vancouver, B. C.,
Canada V6T 2A3*
(October 19, 1994)

Abstract

The role of the relativistic amplitudes for a number of $\mathcal{O}(k)$ processes usually neglected in potential model calculations of NN-bremsstrahlung is investigated. In particular, we consider the Δ -excitation pole contributions related to the one-pion and one-rho exchange and in addition include the exchange contributions induced by the radiative $\omega, \rho \rightarrow \pi\gamma$ decays. The contributions are calculated from relativistic Born amplitudes fitted to Δ -production and absorption data in the energy range up to 1 GeV and then used to supplement potential model and soft photon calculations for nucleon-nucleon bremsstrahlung. The effects on $NN\gamma$ -observables, although moderate in general, are found to be important in some kinematic domains.

13.75.Cs, 25.20.-x, 25.40.-h

arXiv:nucl-th/9410040v1 21 Oct 1994

I. INTRODUCTION

Nucleon–nucleon bremsstrahlung has been extensively investigated both experimentally and theoretically during the past 30 years. For $pp \rightarrow pp\gamma$ the experimental data available covers an energy domain between 42 MeV [1] and 730 MeV [2], the most recent results being obtained at incident proton energies around the pion production threshold [3–5]. Up to the pion production threshold, the $NN\gamma$ potential model using realistic NN–potentials for the description of the nuclear force plus first order approximation for the electromagnetic interaction gives the most successful description.

A comparison of different NN–interactions yields widely equivalent $NN\gamma$ –results in the whole kinematic range [6], so that bremsstrahlung provides a sensitive test for the dynamical model used to describe the photon emission. In the framework of the potential model, however, there is little controversy about the basic features and the correction terms to be used. In particular, relativistic spin corrections as derived in [7,8] and rescattering contributions [9] are used in the most recent analyses [6,10], see also [11,12]. Moreover, the role of Coulomb corrections in $pp\gamma$ [13] and exchange currents in the $np\gamma$ cross section have been discussed [9,14].

The main theoretical problems left are presumably related to shortcomings in principle of the potential model description. For example, Lorentz invariance can only be accounted for approximately by a covariant treatment of the kinematic transformations, inclusion of higher order terms in (p/m) in the electromagnetic operator (relativistic spin corrections) and an appropriate description of the NN–interaction. Further common features of existing potential model calculations are the absence of dynamical baryon resonances and the neglect of two–body currents beyond the $\mathcal{O}(k^0)$ terms given by the soft photon approximation (SPA).

The role of the Δ –excitation was studied in the 1970’s in two different approaches. The authors of [15] used a dispersion analysis in order to correct the one–pion exchange neutron–proton electromagnetic current. The effect of the Δ –resonance on the $np\gamma$ cross section at 200 MeV turned out to be small. In [16] and [17], the Δ –excitation part of the $pp\gamma$ amplitude was derived from phenomenological Lagrangians and combined with soft photon or one–boson exchange Born calculations for the radiative background.

A more sophisticated potential approach including effects of the Δ based on a coupled channel calculation of the half off–shell NN– and $N\Delta$ T–matrices together with a phenomenological $N\Delta\gamma$ –vertex has been published recently [18,19]. In contrast to the $np\gamma$ –results of [15], the authors find an appreciable Δ contribution to the 280 MeV $pp\gamma$ observables.

For higher energies where the potential model is inappropriate, the closely related problem of dilepton production has recently been studied in the framework of an effective one–boson exchange plus Δ –excitation Born approximation [20].

As mentioned above, a rigorous derivation of induced two–body currents is not possible to all orders. The reason is that, unlike e. g. for a one–pion exchange potential [21], the gauge invariant replacement $V_N(\vec{p}) \rightarrow V_N(\vec{p} - e\vec{A})$ in the argument of a general NN–potential V_N [9,14] leads to an unique expression for the induced current only in SPA. To this order, the induced current approximates contributions due to the exchange of charged mesons and vanishes for $pp\gamma$. The radiative decay processes we are considering here are thus not accounted for in the conventional potential model. So far, only the radiative $\omega \rightarrow \pi^0\gamma$ decay

for $pp\gamma$ has been considered as an example of such an $\mathcal{O}(k)$ internal radiation process [22].

The purpose of the present work is to provide an estimate of the role of baryon resonances and internal radiation processes reliable up to photon energies of about 300 MeV corresponding to the highest photon energy possible in the 730 MeV $pp\gamma$ -experiment of [2]. From a comparison with recent analyses of pion-photoproduction [23], we expect the $\Delta(1232)$ -resonance and the radiative decay of the ω and ρ to be the leading corrections.

A coupled channel calculation for the $NN - N\Delta$ system omitting the contribution of the $\Delta\Delta$ -states [24] is typically represented by a set of Lippmann-Schwinger equations

$$T_{NN} = V_{NN} + V_{NN}G_N T_{NN} + V_{N\Delta}G_\Delta T_{\Delta N}, \quad (1.1)$$

$$T_{\Delta N} = V_{\Delta N} + V_{\Delta N}G_N T_{NN} + V_{\Delta\Delta}G_\Delta T_{\Delta N}. \quad (1.2)$$

Inclusion of the Δ thus modifies the NN-amplitude T_{NN} and yields an additional amplitude $T_{\Delta N}$. The pure NN-interaction below the pion production threshold is known to be well described by phenomenological and/or meson theoretic potentials so that we feel safe identifying T_{NN} of equation (1.1) with a pure NN-T-matrix calculated from a realistic nuclear potential in effect absorbing the $V_{N\Delta}G_\Delta T_{\Delta N}$ piece. By then adding the Δ -excitation Born terms, we basically neglect the modifications of the amplitude $T_{\Delta N}$ (equation (1.2)) induced by the iterative terms. Empirically, i. e. from a comparison of the Born amplitude $V_{\Delta N}$ with coupled channel Δ -absorption predictions for lab energies of 50 – 300 MeV [24], and experimental Δ -production data at 800 MeV [25] and 970 MeV [26], it turns out that the effect of the iteration can be simulated by a simple energy-dependent rescaling of the Born amplitude in good approximation. We are then left basically with possible errors originating from the superposition of a (necessarily real and therefore not unitary) Born amplitude with the iterated potential model and SPA amplitudes. Our approach for the Δ is thus complementary to a full coupled channel calculation [18] which systematically avoids the shortcomings mentioned above but cannot be extended easily to processes such as the internal radiative decays and – at least in the $NN\gamma$ -case – cannot be applied at higher energies.

In the following two sections, a description of the model together with a discussion of the parameters will be given. Results for $pp\gamma$ and $np\gamma$ are presented in section IV. We have taken care to test thoroughly the influence of the experimental and theoretical uncertainties for the various ingredients of the amplitude that can not be fixed to accurate data. The results might be useful to estimate the reliability not only of this but of any comparable calculation.

II. INCLUSION OF THE Δ

For the derivation of the Δ -excitation terms depicted in Fig. 1 we start from the interaction Lagrangians for the isovector mesons π and ρ (see [27]) in the notation of [28]:

$$\mathcal{L}_{\pi NN} = -ig_{\pi NN}\bar{\psi}\gamma_5\vec{\tau}\psi\vec{\pi} \quad (2.1)$$

$$\mathcal{L}_{\rho NN} = -g_{\rho NN}\left(\bar{\psi}\gamma^\mu\vec{\tau}\psi\vec{\rho}_\mu + \frac{\kappa_\rho}{4m_N}\bar{\psi}\sigma^{\mu\nu}\vec{\tau}\psi(\partial_\mu\vec{\rho}_\nu - \partial_\nu\vec{\rho}_\mu)\right) \quad (2.2)$$

$$\mathcal{L}_{\pi N\Delta} = -\frac{g_{\pi N\Delta}}{m_\pi}\bar{\psi}\vec{T}\psi_\Delta^\mu\partial_\mu\vec{\pi} + H.c. \quad (2.3)$$

$$\mathcal{L}_{\rho N\Delta} = i \frac{g_{\rho N\Delta}}{m_\rho} \bar{\psi} \gamma^5 \gamma^\mu \vec{T} \psi_\Delta^\nu (\partial_\mu \vec{\rho}_\nu - \partial_\nu \vec{\rho}_\mu) + H.c., \quad (2.4)$$

where ψ_Δ is the spin-3/2 Rarita-Schwinger field and \vec{T} stands for the isospin operator for the transition of an isospin-1/2 and isospin-1 to an isospin-3/2 particle [27]. We have used the pseudoscalar πNN -coupling for convenience. As the πNN -vertices in our calculations involve only on-shell nucleons, pseudovector coupling for the pion instead of equation (2.1) would not change any of our results. From eq. (2.1) – (2.4), the vertex functions read

$$\begin{aligned} \Lambda_{\pi NN} &= g_{\pi NN} \gamma_5, & \Lambda_{\rho NN}^\mu(q) &= -i g_{\rho NN} \left(\gamma^\mu - \frac{\kappa_\rho}{2m_N} i \sigma^{\mu\nu} q_\nu \right), \\ \Lambda_{\pi N\Delta}^\mu(q) &= \frac{g_{\pi N\Delta}}{m_\pi} q^\mu, & \Lambda_{\rho N\Delta}^{\mu\nu}(q) &= i \frac{g_{\rho N\Delta}}{m_\rho} (\not{q} g^{\mu\nu} - \gamma^\mu q^\nu) \gamma_5 \end{aligned} \quad (2.5)$$

and one derives the transition amplitudes for diagram (a) in Fig. 1 [17]:

$$\begin{aligned} T^{(1)}(p_1, p_2; p_3, p_4) &= \bar{u}(p_3) \Lambda_{\pi N\Delta}^\nu(q) P_{\nu\sigma}^\Delta(p_1 - k) \epsilon_\mu \Gamma_{\gamma N\Delta}^{\mu\sigma}(k, p_1 - k) u(p_1) \\ &\quad P^\pi(q) \bar{u}(p_4) \Lambda_{\pi NN} u(p_2) \\ &\quad + \bar{u}(p_3) \Lambda_{\rho N\Delta}^{\lambda\nu}(q) P_{\nu\sigma}^\Delta(p_1 - k) \epsilon_\mu \Gamma_{\gamma N\Delta}^{\mu\sigma}(k, p_1 - k) u(p_1) \\ &\quad P_{\lambda\tau}^\rho(q) \bar{u}(p_4) \Lambda_{\rho NN}^\tau u(p_2), \end{aligned} \quad (2.6)$$

and equivalently for diagram (b)

$$\begin{aligned} T^{(2)}(p_1, p_2; p_3, p_4) &= \bar{u}(p_3) \epsilon_\mu \tilde{\Gamma}_{\gamma N\Delta}^{\mu\sigma}(k, p_3 + k) P_{\sigma\nu}^\Delta(p_3 + k) \tilde{\Lambda}_{\pi N\Delta}^\nu(q) u(p_1) \\ &\quad P^\pi(q) \bar{u}(p_4) \Lambda_{\pi NN} u(p_2) \\ &\quad + \bar{u}(p_3) \epsilon_\mu \tilde{\Gamma}_{\gamma N\Delta}^{\mu\sigma}(k, p_3 + k) P_{\sigma\nu}^\Delta(p_3 + k) \tilde{\Lambda}_{\rho N\Delta}^{\lambda\nu}(q) u(p_1) \\ &\quad P_{\lambda\tau}^\rho(q) \bar{u}(p_4) \Lambda_{\rho NN}^\tau u(p_2). \end{aligned} \quad (2.7)$$

Here, the energies and momenta are constrained according to $p_1 + p_2 = p_3 + p_4 + k$, $q = p_4 - p_2$ is the four momentum transferred by the meson, ϵ_μ the photon unit polarization vector, u, \bar{u} denote free nucleon Dirac spinors and P the appropriate propagators for the mesons and the Δ . With the tilde in equation (2.7) we indicate that the vertex function has to be taken from the Hermitian conjugate of the corresponding Lagrangian.

Associated with eqs. (2.6) and (2.7) are isospin factors, e. g. in case of proton-proton bremsstrahlung:

$$\langle \chi_p | T_3 | \chi_{\Delta^+} \rangle \langle \chi_{\Delta^+} | T_3 | \chi_p \rangle \langle \chi_p | \tau_3 | \chi_p \rangle = \frac{2}{3}$$

The full Δ excitation amplitude including the isospin factors and a relative minus for graphs involving interchange of the final state particles is then

$$\begin{aligned} T_\Delta^{pp\gamma} &= \frac{2}{3} \sum_{i=1}^2 \left\{ T^{(i)}(p_1, p_2; p_3, p_4) + T^{(i)}(p_2, p_1; p_4, p_3) \right. \\ &\quad \left. - (T^{(i)}(p_1, p_2; p_4, p_3) + T^{(i)}(p_2, p_1; p_3, p_4)) \right\} \\ T_\Delta^{np\gamma} &= \frac{2}{3} \sum_{i=1}^2 \left\{ (-T^{(i)}(p_1, p_2; p_3, p_4) + T^{(i)}(p_2, p_1; p_4, p_3)) \right. \\ &\quad \left. + (-1)^{(i)} (-T^{(i)}(p_1, p_2; p_4, p_3) + T^{(i)}(p_2, p_1; p_3, p_4)) \right\}. \end{aligned} \quad (2.8)$$

For the electromagnetic $N\Delta$ current of diagram (a) we use the parametrization [29]

$$\Gamma_{\gamma N\Delta}^{\mu\nu}(k, p) = -ie \left\{ \frac{G_1}{m_N} (\gamma^\mu k^\nu - \not{k} g^{\mu\nu}) + \frac{G_2}{m_N^2} (p^\mu k^\nu - k \cdot p g^{\mu\nu}) \right\} \gamma_5. \quad (2.9)$$

$\tilde{\Gamma}_{\gamma N\Delta}(k, p)$ is equal to $\Gamma_{\gamma N\Delta}(k, p)$ up to a relative minus sign in the term proportional to G_1 . The couplings G_1 and G_2 are experimentally determined by a fit to the $M1^+/E1^+$ multipole pion-photoproduction cross section. Values for G_1 and G_2 range from $G_1 = 2.0$, $G_2 = 0$, the prediction of the vector dominance model, to $G_1 = 2.68$, $G_2 = -1.84$ [18,29], recently quoted values being $G_1 = 2.208$, $G_2 = -0.556$ [23].

The choice of the Δ -propagator requires some caution. In [17], the Rarita-Schwinger form

$$P_\Delta^{\mu\nu}(p) = \frac{\not{p} + m_\Delta}{p^2 - m_\Delta^2 + i\Gamma m_\Delta} \left(g^{\mu\nu} - \frac{1}{3} \gamma^\mu \gamma^\nu - \frac{2}{3} \frac{p^\mu p^\nu}{m_\Delta^2} - \frac{\gamma^\mu p^\nu - p^\mu \gamma^\nu}{3m_\Delta^2} \right), \quad (2.10)$$

is used where the replacement $m_\Delta \rightarrow m_\Delta - i\Gamma/2$ is made in order to account for inelasticities due to pion production. As we wish to use P_Δ in the far off-resonance region ($p^2 \ll m_\Delta$), we have to take the energy dependence of the width $\Gamma \rightarrow \Gamma(q)$ into account. For our purpose, we rely on the parametrization of [30] requiring Γ to vanish below the pion production threshold:

$$\begin{aligned} \Gamma(q_{\pi N}) &= 0, \quad q^2 \leq 0, \quad q_{\pi N} \equiv |\vec{q}_{\pi N}| \\ \Gamma(q_{\pi N}) &= 2\gamma(q_{\pi N} R/m_\pi)^3 / (1 + (q_{\pi N} R/m_\pi)^2), \quad q_{\pi N}^2 > 0. \end{aligned} \quad (2.11)$$

Here, $q_{\pi N}$ denotes the maximum momentum in the πN -subsystem of the process $NN \rightarrow NN\pi$:

$$\begin{aligned} q_{\pi N}^2 &= (s_{\pi N} - (m_\pi - m_N)^2)(s_{\pi N} - (m_\pi + m_N)^2) / 4s_{\pi N}, \\ s_{\pi N} &= (\sqrt{s} - m_N)^2, \end{aligned} \quad (2.12)$$

\sqrt{s} is the invariant energy in the NN -system and R , γ are adjustable parameters. Values of $\gamma = 0.71 \text{ MeV}$, $R = 0.81$ lead to a resonance width $\Gamma = 120 \text{ MeV}$ at $s_{\pi N} = 1236 \text{ MeV}$ [30]. This value might be slightly modified by a variation of γ . It has been shown [31] that this parametrization is in good agreement with the experimental δ_{33} phase as well as with a Δ self energy calculation [24].

$NN - N\Delta$ potential models differ in the choice of the Δ -coupling constants as well as in the definition of the meson propagators and vertex form factors. We use these models as a starting point for our calculation defining the Δ -excitation amplitude up to a normalization. In a reliable calculation, the final results should not depend too much on the underlying parameter sets provided they agree comparably well with the empirical NN -data. We therefore compare two different recent coupled channel models: The OBE-model of [24], denoted as model A, and a coupled channel version of the Bonn potential (model I of [27], p. 353), denoted as model B. For model A, we use the meson propagators

$$P^{(\pi)} = \frac{i}{q^2 - m_\pi^2}; \quad P_{\mu\nu}^{(\rho)} = i \frac{-g_{\mu\nu} + q_\mu q_\nu / m_\rho^2}{q^2 - m_\rho^2}. \quad (2.13)$$

The second term in $P^{(\rho)}$ drops out in the calculations of this and the following section. The propagators of model B take the mass difference between the nucleon and the Δ into account:

$$\begin{aligned}
P^{(\pi)} &= -i \left\{ \frac{1}{2\omega_\pi^2} + \frac{1}{2\omega_\pi(m_\Delta - m_N + \omega_\pi)} \right\}; \quad \omega_\pi \equiv \sqrt{m_\pi^2 - q^2}, \\
P_{\mu\nu}^{(\rho)} &= -i \left(-g_{\mu\nu} + q_\mu q_\nu / m_\rho^2 \right) \left\{ \frac{1}{2\omega_\pi^2} + \frac{1}{2\omega_\pi(m_\Delta - m_N + \omega_\pi)} \right\},
\end{aligned} \tag{2.14}$$

In writing down the Lorentz invariant propagators (2.13) and (2.14) we have dropped the static approximation $q^2 \rightarrow -\vec{q}^2$ of the potential models A and B. As we are far from the pole in all our geometries and rescale our final amplitudes this has very little effect on the end results.

For the calculations using model A, each $NN\pi/NN\rho$ -vertex is multiplied by a monopole cutoff $\Lambda_{\pi/\rho}^2/(\Lambda_{\pi/\rho}^2 - q^2)$ and a dipole cutoff $[\Lambda_{\Delta\pi/\rho}^2/(\Lambda_{\Delta\pi/\rho}^2 + \vec{q}^2)]^2$ applies at the $N\Delta\pi/\rho$ -vertices. Here again, we use Lorentz invariant instead of static expressions. For model B, both the NN - and $N\Delta$ -vertices are regularized by cutoffs $[(\Lambda^2 - m_{\pi/\rho}^2)/(\Lambda^2 - q^2)]^n$ where $n = 1, 2$ for π, ρ exchange respectively.

In general, the relativistic off-shell Δ -particle is allowed to propagate with both spin 3/2 and spin 1/2. This extra freedom is reflected by additional off-shell terms in the interaction Lagrangians; the more general chiral $\pi N\Delta$ -vertex functions corresponding to the propagator (2.10) read [32,33]:

$$\begin{aligned}
\Lambda_{\pi N\Delta}^\mu &= \frac{g_{\pi N\Delta}}{m_\pi} \Theta^{\mu\nu}(Z_\pi) q_\nu; \quad \Lambda_{\rho N\Delta}^{\mu\nu} = i \frac{g_{\rho N\Delta}}{m_\rho} (\not{q} \Theta^{\mu\nu} - \gamma^\mu q_\alpha \Theta^{\alpha\nu}) \gamma_5, \\
\Theta^{\mu\nu}(Z_{\pi/\rho}) &= g^{\mu\nu} - (Z_{\pi/\rho} + \frac{1}{2}) \gamma^\mu \gamma^\nu.
\end{aligned} \tag{2.15}$$

A generalization similar to $\Lambda_{\rho N\Delta}$ (with parameter Z_γ) applies for the (leading) G_1 -term of equation (2.9). The Z -parameters are not well determined either theoretically or experimentally. Whereas the simple coupling scheme corresponding to $Z = -1/2$ is generally preferred in potential models, Olssen and Osypowski [33] find experimental values of $Z_\pi = 0 \pm 1/4$, $Z_\gamma = 1/4 \pm 1/4$. Note that the off-shell parameters do not affect a coupled channel calculation at the OBE level but directly enter the Born amplitude for the bremsstrahlung process where the Δ is off-shell. We therefore rely on the parameters of Table 1 as fixed by NN-data (to all orders of a coupled channel calculation) but check the sensitivity of our results to a variation of Z .

This completes the necessary ingredients for the Δ -excitation part of the bremsstrahlung amplitude (2.8). With the definitions of this chapter we have tried to incorporate as much as possible of the experimental information on the $N\Delta$ excitation channels in the NN-interaction which have become available since the earlier Born calculations [17], [16]. On the other hand, the relativistic approach allows us – in contrast to a pure potential model calculation [18] – to extend the analysis to energies far beyond the pion production threshold.

TABLES

	Model A [24]		Model B [27]	
	$\frac{g^2}{4\pi}$	$\Lambda[\text{MeV}]$	$\frac{g^2}{4\pi}$	$\Lambda[\text{MeV}]$
$NN\pi$	14.16	1140	14.4	1800
$NN\rho$	0.43	1140	0.7	2200
	$\kappa = 5.1$		$\kappa = 6.1$	
$N\Delta\pi$	0.35	910	0.35	920
$N\Delta\rho$	4.0	910	19.0	1140

TABLE I. Meson parameter of model A and B. For the definition of form factors, propagators etc. see text.

III. INCLUSION OF THE RADIATIVE ω/ρ -DECAY

We write the Lagrangian for the coupling of the ω -meson to the nucleons in analogy to equation (2.2):

$$\mathcal{L}_{\omega NN} = -g_\omega \left(\bar{\psi} \gamma^\mu \psi \omega_\mu + \frac{\kappa_\omega}{4m_N} \bar{\psi} \sigma^{\mu\nu} \psi (\partial_\mu \omega_\nu - \partial_\nu \omega_\mu) \right), \quad (3.1)$$

and parametrize the radiative decay vertices as in [23]

$$\mathcal{L}_{\omega\pi\gamma} = g_{\omega\pi\gamma} \varepsilon_{\nu\rho\sigma\delta} (\partial^\sigma A_\gamma^\rho) (\partial^\nu \pi^0) \omega^\delta \rightarrow \Lambda_{\rho\delta}^{\omega\pi\gamma}(k, q) = -i g_{\omega\pi\gamma} \varepsilon_{\nu\rho\sigma\delta} k^\sigma q^\nu, \quad (3.2)$$

$$\mathcal{L}_{\rho^i\pi\gamma} = g_{\rho^i\pi\gamma} \varepsilon_{\nu\rho\sigma\delta} (\partial^\sigma A_\gamma^\rho) (\partial^\nu \pi^i) \rho^{i,\delta}; \quad i = 0, +, -. \quad (3.3)$$

With the meson propagators as in (2.13) and a vertex function $\Lambda_{\omega NN}^\mu$ as in eq. (2.5) this yields for the diagram (c) of Fig. 1

$$\begin{aligned} T_{\omega\pi\gamma}^{(c)}(p_1, p_2; p_3, p_4) &= \bar{u}(p_3) \Lambda_\mu^{\omega NN}(p_3 - p_1) u(p_1) P_{(\omega)}^{\mu\delta}(p_3 - p_1) \Lambda_{\delta\rho}^{\omega\pi\gamma}(k, p_4 - p_2) \epsilon_\gamma^\rho \\ &\times P_{(\pi)}(p_4 - p_2) \bar{u}(p_4) \gamma_5 u(p_2), \end{aligned} \quad (3.4)$$

and consequently (see equation (2.8))

$$\begin{aligned} T_{\omega\pi\gamma}^{pp\gamma} &= T(p_1, p_2; p_3, p_4) + T(p_2, p_1; p_4, p_3) \\ &\quad - (T(p_1, p_2; p_4, p_3) + T(p_2, p_1; p_3, p_4)), \\ T_{\omega\pi\gamma}^{np\gamma} &= T(p_1, p_2; p_3, p_4) - T(p_2, p_1; p_4, p_3). \end{aligned} \quad (3.5)$$

The ρ -decay amplitudes are obtained from $T_{\omega\pi\gamma}$ by interchange of the masses and coupling constants and multiplication with the isospin operator $\vec{\tau}_1 \cdot \vec{\tau}_2$. The matrix elements of this operator yields factors of 1 and 0 for the neutral and charged pion decay amplitude in $pp\gamma$. For $np\gamma$ the corresponding values are -1 and 2.

The coupling constants $g_{\omega\pi\gamma}$ and $g_{\rho\pi\gamma}$ are determined from the experimental decay widths of the vector mesons [34]:

$$\Gamma(\omega/\rho \rightarrow \pi\gamma) = \frac{g_{\omega/\rho\pi\gamma}^2}{96\pi} \frac{(m_{\omega/\rho}^2 - m_\pi^2)^3}{m_{\omega/\rho}^3} = \begin{cases} 716 \pm 75 \text{ keV} & \text{for } \omega, \\ 121 \pm 31 \text{ keV} & \text{for } \rho^0, \\ 68 \pm 7 \text{ keV} & \text{for } \rho^\pm. \end{cases} \quad (3.6)$$

This leads to the numerical values

$$\frac{g_{\omega\pi\gamma}^2}{4\pi} = 0.715 \cdot 10^{-3} m_\pi^{-2}; \quad \frac{g_{\rho^0\pi\gamma}^2}{4\pi} = 0.125 \cdot 10^{-3} m_\pi^{-2}; \quad \frac{g_{\rho^\pm\pi\gamma}^2}{4\pi} = 0.070 \cdot 10^{-3} m_\pi^{-2}. \quad (3.7)$$

For the remaining coupling constants and cutoffs, we again follow the rationale of the previous section and use a complete set that has been successfully tested in pion-photoproduction [23]. Thus we put

$$\frac{g_\rho^2}{4\pi} = 0.563; \quad \kappa_\rho = 3.71; \quad \frac{g_\omega^2}{4\pi} = 5.07; \quad \kappa_\omega = -0.12. \quad (3.8)$$

These values are in agreement with the quark model and the vector dominance assumption. All form factors in this section are set to 1; the pion couplings are taken from table 1. Note that a measurement of the vector meson radiative decay contributions in the pion photoproduction process determines the product of the couplings in eqs. (3.7) and (3.8). With the well-known empirical value of g_π , the amplitude (3.4) is therefore essentially fixed.

IV. RESULTS

As mentioned earlier, the amplitudes (2.8) and (3.4) must be divided by an energy dependent scaling factor $g(T_{lab})$ in order to compensate for neglecting higher order terms in the Born series. From a comparison of our Born results using model A with the total Δ -absorption cross sections of [24] calculated in the iterated coupled channel model, one finds a factor $g = 1.65$ at lab energies below 300 MeV. A calculation of the total Δ -production cross section and comparison with the experimental data at 800 MeV [25] and 970 MeV [26] suggests a weak energy dependence of g so that $g(730 \text{ MeV}) = 1.4$. The latter value is in close agreement with the result of [20]. As we have to compensate also for the change from static to Lorentz invariant propagators in eqs. (2.13), (2.14), we use $g(280 \text{ MeV}) = 1.95$ and $g(730 \text{ MeV}) = 1.65$ respectively.

If we suppose the higher order corrections to be of equal importance for both model A and B and for the ω/ρ -decay amplitudes for which no experimental comparison could be made, the model is completely determined with the empirical values of $g(T_{lab})$ found above. The rescaled amplitudes (2.8) and (3.4) can thus be coherently added to the corresponding transition matrices of the potential model [6] and the soft-photon approximation [35,36] so that the effects upon both cross sections and spin observables can be studied. The relevant formula for the observables considered can be found in the literature ([8,17]). For the potential model calculations we shall focus on the domain around pion production threshold where both correction effects should be maximum; the soft photon model will be used to reanalyze the experimental data of [2].

In principle, with all conventions carefully chosen, the formulas in the last two sections give the correct relative signs for the corrections with respect to the leading (potential model or SPA) amplitudes. For an independent check we combined our amplitudes (2.8) and (3.4) with the pure one-pion exchange bremsstrahlung amplitude (Fig. 1, diag. (a) with the internal Δ -line replaced by a nucleon line). If the exchanged pion is numerically put on-shell ($q^0 \rightarrow \sqrt{\vec{q}^2 + m_\pi^2}$), this is equal up to a common factor to the pion-photoproduction amplitude with and without intermediate Δ excitation. In a near-threshold geometry ($\vec{q}^2 \sim 0$), the Δ -amplitude gives enhancement of the cross section by a few percent, in agreement with Peccei's chirally invariant Lagrangian for $\pi^0 p \rightarrow p\gamma$ [37] whereas the ω/ρ -decay amplitudes interfere destructively, as in [23].

The sign of the ω -coupling constant given in eq. (3.7) is consistent with the pion-photoproduction data [23]. The sign of the much smaller radiative ρ -decay amplitude, however, is still the object of controversies [38]. We adopt here the sign convention of Gari et al. [39] where the ρ -decay enhances the contribution of the ω -decay in $pp\gamma$; as the ρ -contribution is only about 2 % of the ω (compare the respective coupling constants), a switch in the sign of $g_{\rho\pi\gamma}$ would not alter our conclusions.

A. Potential Model Results

All the calculations in this section are based on the inversion potential to the Nijmegen-II NN-phase shifts used in Ref. [6]. Using another realistic NN-potential would not change any of our results. The basic features of the potential model can be essentially represented

in terms of two variables: the total energy of the process T_{lab} as a crucial parameter for the relative size of the various contributions in the amplitude, and the opening angles of the two protons determining the maximum photon energy and thus the off-shell signature of the process [6]. The two examples of Fig. 2 show the coplanar, exclusive $pp\gamma$ cross section $d^3\sigma/d\Omega_1 d\Omega_2 d\theta_\gamma$ and the analyzing power A_y for the smallest and largest outgoing proton angle pairs measured in the $T_{lab} = 280$ MeV TRIUMF experiment [3]. The plots show that both Δ -excitations and internal radiative decay contributions are small for the cross section at small proton angles as well as for the analyzing power A_y at large proton angles. The Δ -contribution is the leading effect but tends to be partly cancelled by the radiative decay contributions. The maximum net effect of both contributions can increase the differential cross section by 15 – 20% at medium photon angles but amounts to only a few percent in the total cross section.

Among the examples of Fig. 2, only the 12.4^0 , 14^0 analyzing power shows a sizeable dependence on the parametrization of the π and ρ -exchange. The choice of different electromagnetic couplings, e. g. $G_1 = 2.68$, $G_2 = -1.84$, increases the Δ -contribution in the cross sections by about 20 % which translates to an enhancement of the complete $pp\gamma$ cross section by about 5 % at maximum (Figure 3). Conversely, the choice of $Z_\pi = Z_\gamma = -1/4$ [23] reduces the size of the Δ -contributions by roughly 20%. These two choices for the couplings and off-shell parameters are likely to be rather extreme. Moreover, because of its small relative size, a rescaling error in the ω/ρ -amplitude would not affect much the end results. One might therefore conclude that the corrections are reasonably well determined in our model.

In order to obtain a more general picture we calculate the double differential cross section $d\sigma/d\Omega_1 d\Omega_2 = \int d\theta_\gamma (d\sigma/d\Omega_1 d\Omega_2 d\theta_\gamma)$ and represent its relative enhancement due to the correction terms as a function of the symmetric angle $\theta = \theta_1 = \theta_2$ (Figure 4). Note that small θ values correspond to a suppression of the meson four momentum transfer ($q \rightarrow 0$) whereas for large θ , the elastic limit $k \rightarrow 0$ is reached. In both cases, the amplitudes (2.8) and (3.4) are suppressed: they are maximum in the medium proton angle region $\theta \sim 20^0$. The relative size of the corrections dies down as the energy decreases and reaches only about 3% at $T_{lab} = 200$ MeV.

In Figure 5 the analysis of Fig. 2 is repeated for the $np\gamma$ -observables. Here, the isospin factors yield strong destructive interference between the various Feynman graphs so that both the Δ excitation and the radiative decays become negligible corrections to the potential model cross section. The same result holds for the $np\gamma$ -analyzing power. We thus confirm the result of [15] that Δ -corrections to the $np\gamma$ -amplitude are weak.

B. 730 MeV (SPA) Results

Two typical geometries of the 730 MeV $pp\gamma$ -experiment reported in Ref. [36] are shown in Fig 5. One proton is emitted at $\theta_1 = 50.5^0$, $\phi_1 = 0^0$ and the polar angles of the photon are $\theta_\gamma = 67^0$, $\phi_\gamma = 179^0$ for counter G7 and $\theta_\gamma = 54^0$, $\phi_\gamma = 131^0$ for counter G10. The solid curves have been obtained with the soft photon approximation of [35]. Contributions in $\mathcal{O}(k)$ are only partly included in SPA; the corrections considered here are thus specific candidates for the missing $\mathcal{O}(k)$ effects.

As expected the corrections are negligible for small k but increase with the photon energy. Analogous to the 280 MeV examples, there is cancellation between the Δ - and ω/ρ -effects. The actual size is again geometry dependent but is limited to about 20% of the SPA cross section at $k = 150$ MeV. A variation of the electromagnetic coupling constants and off-shell parameters within the experimental limits yields effects analogous to those shown in Fig. 3 and leaves a freedom of a few percent in our final $k = 150$ MeV results. Correspondingly, the results are not much altered by interchange of model A and B. We conclude that a Δ -amplitude consistent with experimental results can only resolve a small part of the discrepancy between the SPA and the 730 MeV $pp\gamma$ -results at photon energies above ~ 100 MeV.

V. CONCLUDING REMARKS

We have evaluated the Δ -excitation and radiative ω/ρ -decay corrections to proton-proton and neutron-proton bremsstrahlung for the energy range up to $T_{lab} \sim 1$ GeV. This was done by calculating the relativistic Born amplitudes and adding them to potential model and SPA amplitudes. The Born amplitudes were normalized by calculating Δ -production and absorption cross sections in the same model and fitting to experimental data and coupled channel predictions.

Of the two processes considered, the Δ -excitation dominates but is generally partly compensated by the radiative decay contributions. Both corrections together increase the 280 MeV $pp\gamma$ integrated cross section $d^2\sigma/d\Omega_1d\Omega_2$ by an amount depending essentially on the proton opening angles θ_i and reaching a maximum of roughly 7.5% at $\theta_1 \sim \theta_2 \sim 20^\circ$. The relative effect on $d^3\sigma/d\Omega_1d\Omega_2d\theta_\gamma$ is maximum for photon emission around $\theta_\gamma = 90^\circ$ and is typically $\leq 20\%$.

In the 730 MeV Rochester geometry, the corrections become relevant for photon energies above ~ 100 MeV but are not big enough to complement the soft photon approximation and fit the experimental data [36].

We have taken care to study and discuss the limits and uncertainties of our model. The results have been obtained on the basis of two different parametrizations of the Δ -excitation (model A and B of Table 1) but show little sensitivity to the underlying coupled-channel model. The fact that the Δ -excitation cross sections of Model A and B are nearly identical, despite the rather massive differences in the values of the ρ -couplings and the choice of form factors and propagators, is reassuring for our approach but corresponds to the result obtained earlier that rather different potential models, once they fit the NN-scattering data, yield very similar bremsstrahlung results [6] and is disappointing if one hopes to understand the underlying physical reaction mechanism from $NN\gamma$ measurements.

The experimental uncertainty in the radiative Δ -decay constants and the off-shell freedom of the Δ suggest a theoretical error of about $\pm 20\%$ in the final correction amplitudes, i. e. up to $\sim \pm 4\%$ in the total (280 MeV) $pp\gamma$ cross section. We should mention that the discrepancies between the $pp\gamma$ predictions of different NN-potential models, which most bremsstrahlung experiments in the past were designed to isolate, are of the same order of magnitude. Given the present experimental status of nucleon-nucleon bremsstrahlung and the theoretical ambiguities mentioned, it is not possible to use $NN\gamma$ -data for putting limits

on the parameters entering our correction amplitudes.

In view of the similarities of our calculation with previous ansatzes, a comprehensive comparison of the results seems worthwhile. First note that we have eliminated the uncertainty with respect to the relative sign of the relativistic corrections stated by Kamal and Szyjewicz [22] through a comparison with the pion–photoproduction process. Our ω/ρ –decay amplitude extends the amplitude of [22] by including the ω –tensor coupling terms and the ρ –decays and is, if we divide by $g(T_{lab})$, slightly smaller than given there.

The discrepancy of our result is more serious for the 730 MeV Δ –excitation calculation where the previous authors lack a reliable model for the NN–channel $pp\gamma$ –amplitude. The authors of [17] therefore essentially fit the Δ –excitation part to the experimental $pp\gamma$ data. In [16], the suppression of the amplitude which we simulate by appropriate form factors is neglected. In both cases, the pure Δ –cross section becomes bigger than ours by more than a factor of 10 and would be in clear contradiction to the 800 MeV Δ –production data of, e. g. [25]. We also stress the importance of taking interference terms correctly into account.

The dispersion theoretic approach used in [15] to estimate the role of the Δ –resonance in a OPE– $np\gamma$ calculation is rather different from our model. Correspondingly, the results agree only in relative size.

Finally, a comparison with the coupled–channel Δ –results of [18] in the low energy region shows good agreement for the cross sections and even for the analyzing powers A_y . This is encouraging for the feasibility of our method as well as for the various extensions made.

We wish to thank Dr. S. Scherer for valuable discussions. This work was supported in part by a grant from the Natural Sciences and Engineering Research Council of Canada.

REFERENCES

- [1] C. A. Smith, J. V. Jovanovich and L. G. Greeniaus, Phys. Rev. **C22** (1980), 2287 and earlier publications quoted therein.
- [2] B. M. K. Nefkens, O. R. Sander and D. I. Sober, Phys. Rev. Lett. **38** (1977), 876
- [3] K. Michaelian et al., Phys. Rev. **D41**, 2689 (1990)
- [4] P. Kitching et al., Phys. Rev. Lett. **57**, 2363 (1986); Nucl. Phys. **A463**, 87 (1987)
- [5] B. v. Przewoski et al., Phys. Rev. **C45**, 2001 (1992)
- [6] M. Jetter and H. V. von Geramb, Phys. Rev. **C49**, 1832 (1994). See also: M. Jetter, H. Freitag und H. V. von Geramb, Nucl. Phys. **A553**, 655c (1993) and Phys. Scr. **48**, 228 (1993)
- [7] R.L. Workman and H. W. Fearing, Phys. Rev. **C34**, 780 (1986)
- [8] M. K. Liou and M. E. Sobel, Ann. Phys. **72**, 323 (1972)
- [9] K. Nakayama, Phys. Rev. **C39**, 1475 (1989)
- [10] V.A. Herrmann and K. Nakayama, Phys. Rev. **C45**, 1450 (1992), V. Herrmann, J. Speth and K. Nakayama, Phys. Rev. **C43**, 394 (1991)
- [11] V. Brown, P. L. Anthony and J. Franklin, Phys. Rev. **C44**, 1296 (1991)
- [12] A. Katsogiannis and K. Amos, Phys. Rev. **C47**, 1376 (1993)
- [13] A. Katsogiannis, K. Amos, M. Jetter and H. V. von Geramb, Phys. Rev. **C49**, 2342 (1994)
- [14] V.R. Brown and J. Franklin, Phys. Rev. **8**, 1706 (1973)
- [15] G. E. Bohannon, L. Heller and R. H. Thompson, Phys. Rev. **C16**, 284 (1977)
- [16] A. Szyjewicz and A. N. Kamal, in: *Few Body Systems and Nuclear Forces I (Proc., Graz 1978)*, ed. by H. Ziegler, M. Haftel and H. Zankel; A. Szyjewicz and A. N. Kamal, in: *Nucleon–Nucleon Interactions (Proc., Vancouver 1977)*, ed. by H. Fearing, D. Measday and A. Strathdee, AIP conf. proc. no. 41 (1978)
- [17] L. Tiator, H. J. Weber and D. Drechsel, Nuc. Phys. **A306**, 468 (1978),
- [18] F. de Jong, K. Nakayama, V. Herrmann and O. Scholten, Phys. Lett. **B333**, 1 (1994)
- [19] J. A. Eden et al. have recently performed a potential model calculation of Δ -effects in proton–proton bremsstrahlung (private communication).
- [20] M. Schäfer et al., Nucl. Phys. **A575**, 429 (1994)
- [21] D. O. Riska, Phys. Rep. **181**, 207 (1989)
- [22] A. N. Kamal and A. Szyjewicz, Nucl. Phys. **A285**, 397 (1977)
- [23] H. Garcilazo and E. M. de Goya, Nucl. Phys. **A562**, 521 (1993)
- [24] B. ter Haar and R. Malfliet, Phys. Rep. **149**, 208 (1987)
- [25] J. Hudomalj–Gabitzsch et al., Phys. Rev. **C6**, 2666 (1978)
- [26] V. Dmitriev, O. Sushkov and C. Gaarde, Nucl. Phys. **A459**, 503 (1986)
- [27] R. Machleidt, in *Advances in Nuclear Physics, Vol. 19*, J. W. Negele and E. Vogt ed., (1989)
- [28] J. D. Bjorken and S. D. Drell, *Relativistic Quantum Mechanics*, McGraw–Hill, New York (1964)
- [29] H. F. Jones and M. D. Scadron, Ann. Phys. **81**, 1 (1973)
- [30] E. E. van Faassen and J. A. Tjon, Phys. Rev. **C28**, 2354 (1983)
- [31] E. E. van Faassen and J. A. Tjon, Phys. Rev. **C33**, 2105 (1986)
- [32] R. Wittman, Phys. Rev. **C37**, 2075 (1988)

- [33] M. G. Olsson and E. T. Osypowski, Nucl. Phys. **B87**, 399 (1975)
- [34] Particle Data Group, Phys. Rev. **D45**, part II (1992)
- [35] H. W. Fearing, Phys. Rev. **C 6**, 1136 (1972); H. W. Fearing, in: *Nucleon–Nucleon Interactions (Proc., Vancouver 1977)*, ed. by H. Fearing, D. Measday and A. Strathdee, AIP conf. proc. no. 41 (1978)
- [36] B. M. K. Nefkens, O. R. Sander, D. I. Sober and H. W. Fearing, Phys. Rev. **C19**, 877 (1979)
- [37] R. D. Peccei, Phys. Rev. **181**, 1902 (1969)
- [38] P. Sarriguren, J. Martorell and D. W. L. Sprung, Phys. Lett. **B228**, 285 (1989)
- [39] M. Gari and H. Hyuga, Nucl. Phys. **A264**, 409 (1976)

FIGURES

FIG. 1. Δ -excitation and internal radiation processes considered in this text.

FIG. 2. Coplanar $pp\gamma$ exclusive cross sections and analyzing powers at $T_{lab} = 280$ MeV and for the smallest and largest proton angle pairs θ_1, θ_2 of the TRIUMF experiment [3] (the datapoints shown are rescaled with a factor of 0.67 as in this reference). The curves denote the pure potential model of Ref. [6] (solid), potential model plus pure ω/ρ -decay (long dashed), and the full model according to model A (dotted) and B (dashed-dotted).

FIG. 3. Typical uncertainties of the Δ -contribution. The curves show the pure potential model of Ref. [6] (solid) and the full calculation according to model A with standard parameters $G_1 = 2.208, G_2 = -0.278, Z_\pi = Z_\gamma = -1/2$ (long dashed). The upper bound of the shaded area in the cross section and lower bound in A_y corresponds to larger electromagnetic couplings $G_1 = 2.68, G_2 = -1.84$. The lower bound in the cross section and upper bound in A_y is calculated with larger Z -parameters $Z_\pi = Z_\gamma = -1/4$.

FIG. 4. Relative change of the integrated, coplanar $pp\gamma$ cross section $d^2\sigma/d\Omega_1d\Omega_2$ (with corrections)/ $d^2\sigma/d\Omega_1d\Omega_2$ (without corrections) at 280 MeV (dashed), 200 MeV (dashed-dotted) and 157 MeV (dotted) for parameter set A as a function of the symmetric proton angles $\theta_1 = \theta_2$.

FIG. 5. Coplanar $np\gamma$ exclusive cross section and analyzing power at $T_{lab} = 280$ MeV. The curves denote the pure potential model of Ref. [6] (solid), plus pure ω/ρ -decay (long-dashed), and the full model according to model A and B (dashed-dotted and dotted).

FIG. 6. 730 MeV $pp\gamma$ measurements and soft photon approximation in two typical geometries (see [36] (1979) and text). The curves denote the pure SPA results (solid), plus pure ω/ρ -decay (long-dashed), and the full model according to model A (dotted).

This figure "fig1-1.png" is available in "png" format from:

<http://arxiv.org/ps/nucl-th/9410040v1>

This figure "fig2-1.png" is available in "png" format from:

<http://arxiv.org/ps/nucl-th/9410040v1>

This figure "fig1-2.png" is available in "png" format from:

<http://arxiv.org/ps/nucl-th/9410040v1>

This figure "fig2-2.png" is available in "png" format from:

<http://arxiv.org/ps/nucl-th/9410040v1>

This figure "fig1-3.png" is available in "png" format from:

<http://arxiv.org/ps/nucl-th/9410040v1>

This figure "fig2-3.png" is available in "png" format from:

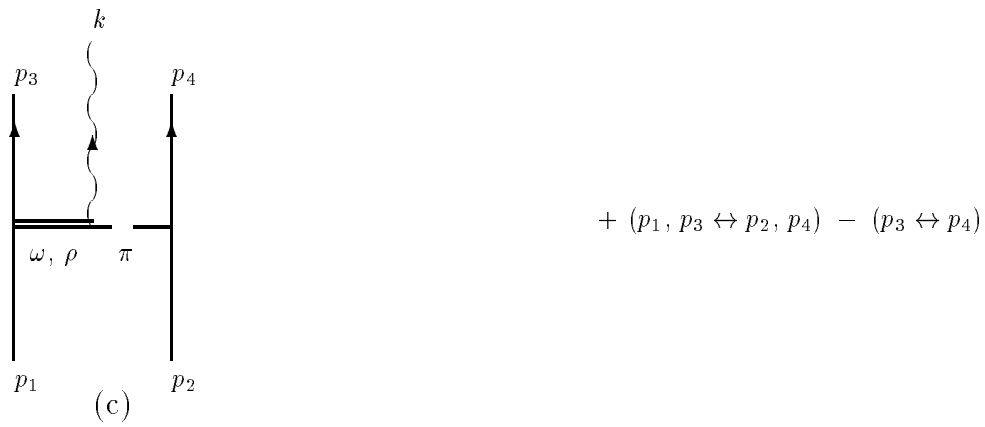
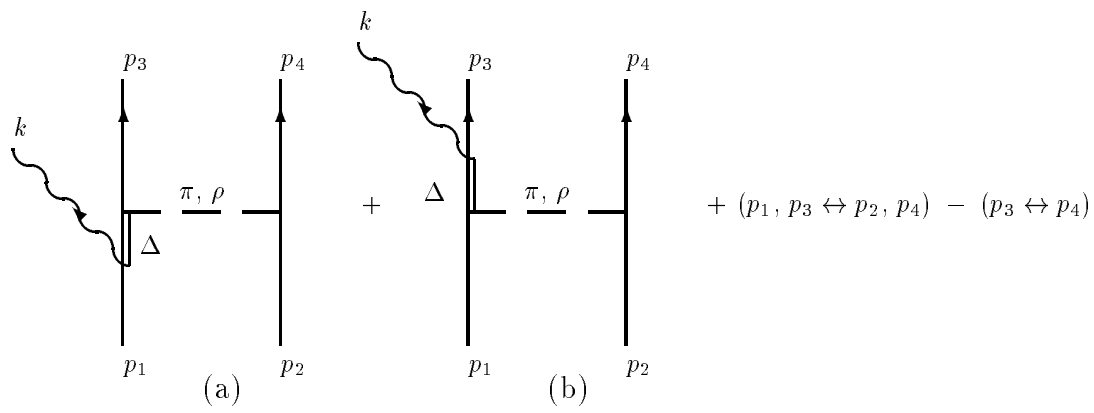
<http://arxiv.org/ps/nucl-th/9410040v1>

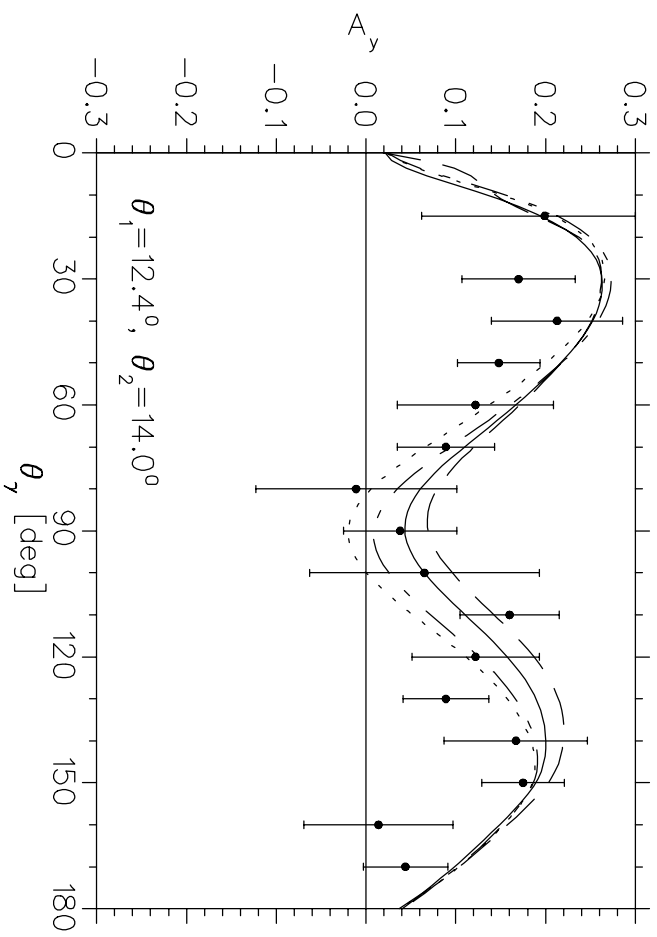
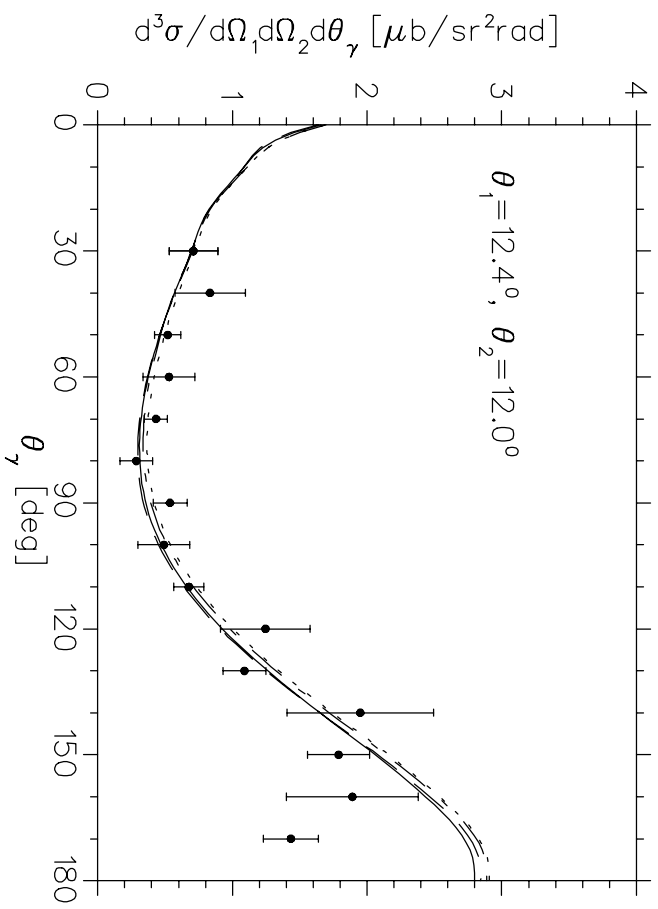
This figure "fig1-4.png" is available in "png" format from:

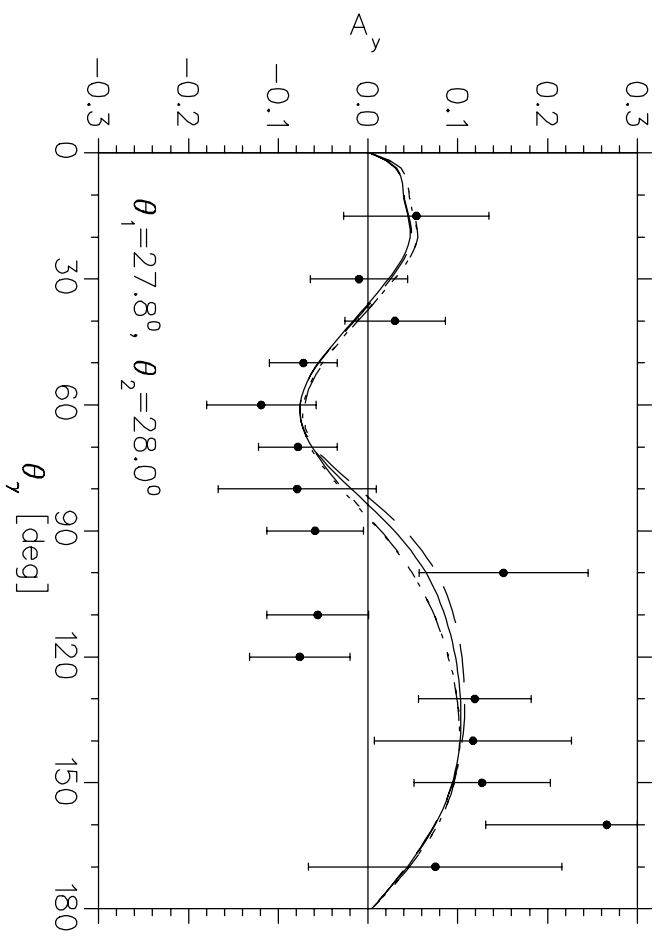
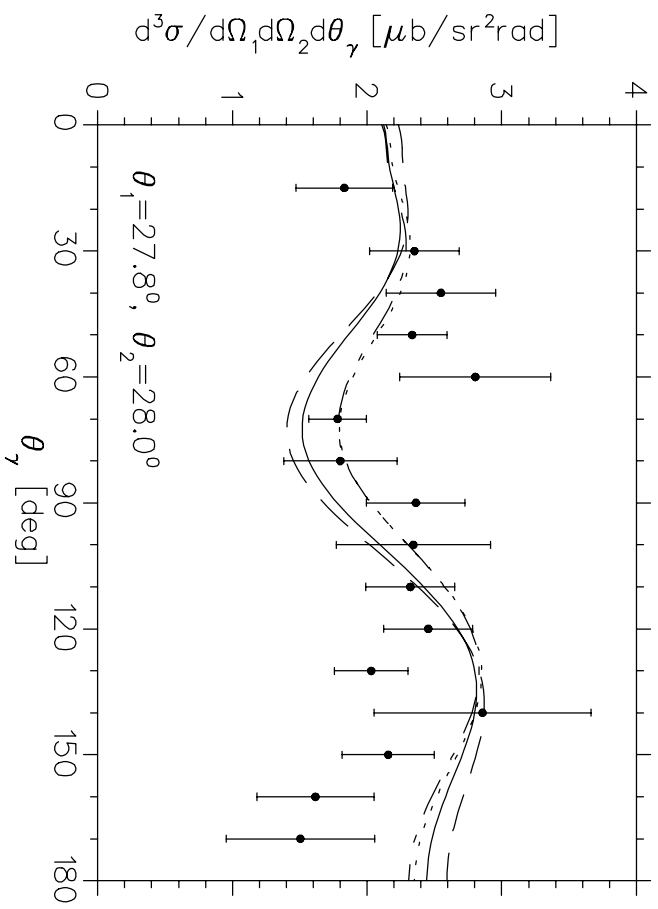
<http://arxiv.org/ps/nucl-th/9410040v1>

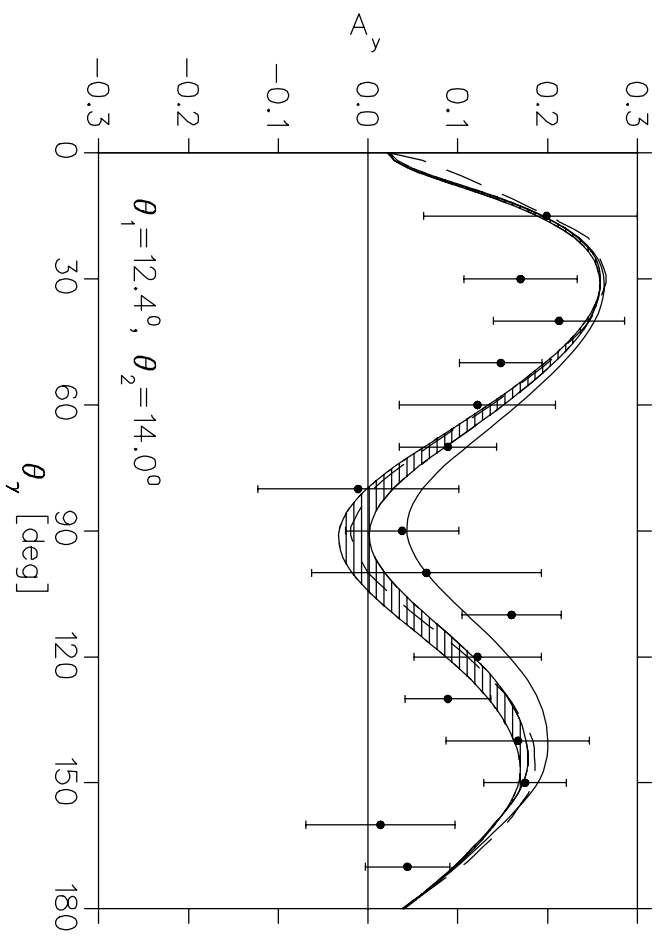
This figure "fig1-5.png" is available in "png" format from:

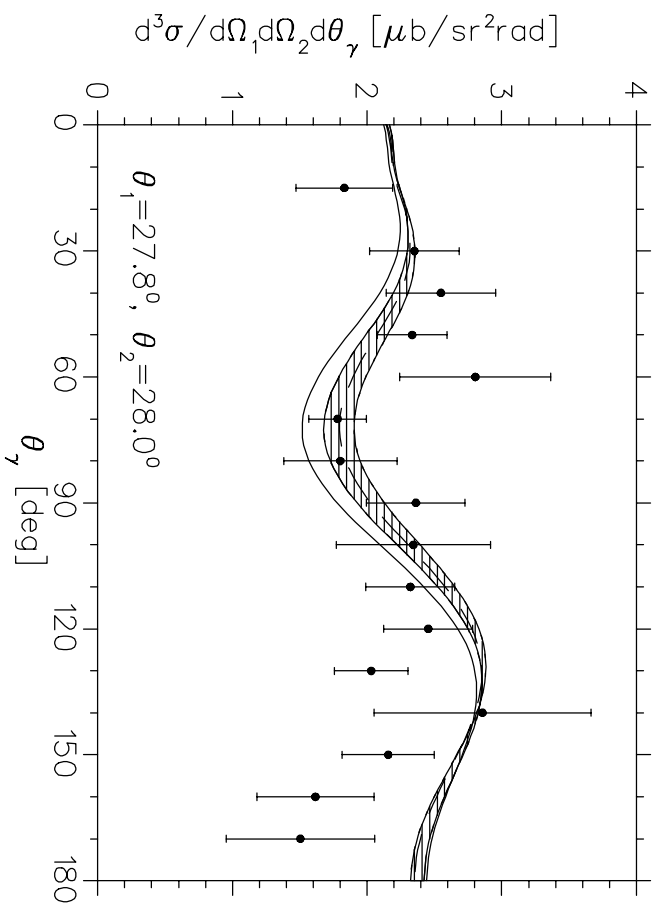
<http://arxiv.org/ps/nucl-th/9410040v1>











Relative Δ and ω/ρ Effects

